

Electronic Supplementary Material

Performance evaluation of a semi-automated method for [¹⁸F]FDG uptake in abdominal visceral adipose tissue

Journal: Molecular Imaging and Biology

*Stefanie A. de Boer¹, *Daan S. Spoor^{2,3}, Riemer H.J.A. Slart^{2,4}, Douwe J. Mulder¹, Melanie Reijrink¹, Ronald J.H. Borra^{2,5,6}, Gerbrand M. Kramer⁷, Otto S. Hoekstra⁷, Ronald Boellaard^{2,7}, Marcel J. Greuter^{4,6}

*Contributed equally to this work.

Address of correspondence

Stefanie A. de Boer, MD, PhD

University Medical Center Groningen, department of Vascular Medicine, HP AA41

Hanzeplein 1

9713 GZ Groningen, Netherlands

Phone number: +31503616161 / Fax number: +31503619069

E-mail address: s.a.de.boer@umcg.nl

LITERATURE SEARCH details

Search strategy and selection criteria

Studies were identified by a search of the PubMed and Embase database using the following keyword: synonyms for [¹⁸F]-2—fluoro-2-deox-D-glucose (FDG) AND synonyms for abdominal fat AND published between 1 January 1995 up to 1 November 2016 (details search strategy are presented in Suppl. Table 1).

To be selected for this review, studies had to fulfill the following eligibility criteria:

(1) [¹⁸F]FDG used as a tracer in PET; (2) [¹⁸F]FDG uptake reported as standardized uptake value (SUV, i.e. the decay-corrected tissue radioactivity concentration divided by the administered dose per body weight); (3) [¹⁸F]FDG uptake reported of adipose abdominal tissue; (4) published in the English language.

Prospective and retrospective studies were included. Reviews, abstracts, editorials, and case reports were excluded from this review. The search revealed 248 papers of which 93 were duplicates, so 155 potentially papers were reviewed (details Suppl. Fig. 1). Reviewing titles and abstract revealed 32 potentially eligible for inclusion. After reviewing the full article, 18 papers were excluded because [¹⁸F]FDG uptake was not reported as SUV or only reported of the thoracic visceral adipose tissue or only the visceral fat area or volume was reported and not the [¹⁸F]FDG uptake. Eventually, 14 studies met all inclusion (details presented in Suppl. Table 2).

Results

SUV parameter and reported values

There are four different parameters to report the [¹⁸F]FDG uptake as a SUV. Maximal SUV (SUV_{max}) reflects the most intense voxel activity within a region of interest (ROI) or volume of interest (VOI). Mean SUV (SUV_{mean}) reflects the mean SUV within the ROI or VOI. The target to background ratio (TBR) is calculated as the ratio of SUV_{max} of the ROI/VOI and venous blood pool SUV_{mean}, to correct for blood-pool uptake and is described as TBR_{max} or the ratio of the SUV_{mean} value and venous blood pool as TBR_{mean}.

In eight studies, [¹⁸F]FDG uptake was reported as SUV_{mean}, in two studies as SUV_{max}, in three studies as TBR_{max}, and one study as TBR_{mean}. In addition, only one study which reported a TBR also reported the blood-pool activity so it was possible to also calculate the background uncorrected SUV value.

Method of measurement

All the included studies used a (LD)CT-scan for anatomic information. Only one study also included healthy individuals who underwent a MR scanning combined with PET. The level of measurement of VAT and SAT differed between the vertebra level Th11-12 and L5/S1. Overall, twelve of the fourteen studies used a manually method by drawing ROIs or selecting VOI on the relevant tissue to measure [¹⁸F]FDG uptake. Although, most of the studies used an automatic method first to segment adipose tissue on CT using a Hounsfield Unit (HU) threshold. The amount of ROIs differed between 3 and 25 but the exact amount of ROIs were not always described in detail. There were only two studies who used an automatic 3D isocontour volume of interest to report [¹⁸F]FDG uptake.

MATERIALS AND METHODS

Segmentation and quantitative assessment of VAT and SAT

The body area was extracted with thresholding. Noise and air were removed from the image by applying a threshold of CT pixel values ≤ 274 HU. Bone, muscle or adipose tissue were defined as pixel values ≥ -274 HU. The CT table was automatically removed by calculation of the filled area of each object (connecting components) in a thresholded (pixel values > 184 HU) binary images. The object with the largest filled area was always the body.

The body area was divided into bone, muscle and adipose tissue compartments. Bone segmentation was performed by thresholding the body region for all pixels ≥ 126 HU, muscle segmentation by thresholding all pixel values of -24 to 126 HU, and adipose tissue by thresholding all pixel values of -174 to -24 HU. These cut-off values were based on previous research (manuscript reference 32-36) and histograms of the LDCT slices. All thresholding was followed by morphological removal of noisy pixels. The sum of the bone and muscle masks formed an adipose tissue mask. The abdominal muscular wall was used as a boundary for the separation of the segmented adipose tissue in VAT and SAT areas. Since on the LDCT the abdominal muscular wall was not always closed, for example at the linea alba, a line to divide VAT and SAT was drawn manually as an extra reference in all slices.

VAT and SAT areas were calculated in every slice by counting the amount of pixels of each segment. By multiplying this area by the spatial resolution of the CT scan the areas in squared centimeter were provided.

Supplementary Tables

Supplemental Table 1 Search strategy and results

Database	Search string	Results
PubMed	("Fluorodeoxyglucose F18"[Mesh] OR FDG[all fields] OR fluorodeoxyglucose[all fields] OR 18FDG [all fields])	113
	AND	
	("abdominal fat"[Mesh] OR (visceral[all fields] AND fat[all fields]) OR (abdom*[all fields] AND fat[all fields]) OR (abdom*[all fields] AND adipose[all fields]) OR (visceral[all fields] AND adipose[all fields]) OR abdominal tissue[all fields] OR visceral tissue[all fields] OR VAT[all fields])	
	AND	
	("1995-01-01"[PDAT]: "2016-11-01"[PDAT])	
Embase	('fluorodeoxyglucose f 18'/exp OR (FDG OR fluorodeoxyglucose OR 18FDG):ab,ti)	135
	AND	
	('abdominal fat'/exp OR ((visceral OR abdom*) AND fat):ab,ti OR ((abdom* OR visceral) AND adipose):ab,ti OR ('abdominal tissue' OR 'visceral tissue' OR VAT):ab,ti)	
	NOT	
	'conference abstract'/it	

Supplemental Table 2: Overview from included studies following literature search

Study	Patients category	Age (years)	N (% males)	BMI	Method/level of SUV measurement	[¹⁸ F]FDG uptake reported as	[¹⁸ F]FDG uptake VAT	[¹⁸ F]FDG uptake SAT
2016 Torigian et al (1)	Heavy smokers and nonsmokers	43±6	20 (100%)	26.2±2.9	The 3D SAT and VAT ROIs generated on CT were transferred to PET images, measurement from the thorax until the pelvis.	SUV _{mean}		
	Chronic heavy cigarette smokers		10 (100%)				0.35±0.10	0.25±0.12
	Nonsmokers (never smokers)		10 (100%)				0.26±0.06	0.22±0.09
2016 Van de Wiele et al (2)	Pancreatic carcinoma	66 (39-80)	38 (66%)	24.6±4.5	ROIs on different slices (lumbal level).	SUV _{mean}	0.6 (range 0.0-1.6)	0.4 (range 0.0-1.0)
2016 Veld et al (3)	MGUS and MM patients	63±11	72 (58%)		ROIs on 4th lumbar vertebra	SUV _{mean}		
	MGUS	64±13	40 (58%)	26.8±3.8			0.22±0.17	0.46±0.20
	MM	62±10	32 (59%)	28.5±5.8			0.85±0.40	0.54±0.73
2016 Pahk et al (4)	Colorectal cancer	64±11.6	131(60%)	?	VAT: ROIs were placed on 3 consecutives slices above or below the kidney. SAT: 3 ROIs: buttock area	SUV _{max}		
	with distant metastasis		13 (?)				1.21±0.39	0.45±0.11
	without distant metastasis		118 (?)				0.76±0.27	0.47±0.15
2016 Im et al (5)	Healthy individuals		49 (59%)		Automatic 3D isocontour VOI using threshold for CT and MR, measurement from the diaphragm to the upper margine of the bladder	SUV _{mean}		
	who underwent FDG PET/CT	54.2±14.7	25 (60%)	23.9±2.9			0.89±0.17	0.53±0.13
	who underwent FDG PET/MR	61.8±13.1	24 (58%)	23.7±2.9			0.50±0.06	0.29±0.06
2015 Bucerius et al (6)	Obese subjects pre and after surgery				VAT: ROIs were placed on 3 consecutives slices above or below the kidney. SAT: ROIs, presternal	TBR _{max}		
	Pre bariatric surgery	40±9	10 (20%)	41.7±4.3			0.65±0.19	0.54±0.30
	After bariatric surgery	41±9	10 (20%)	29.7±4.2			SUV _{max} *: 0.72	SUV _{max} *: 0.59
							SUV _{max} ** : 0.46	SUV _{max} ** : 0.56

* = SUVmax calculated as TBRmax*SUV bloodpool (1.10) ** = SUVmax calculated as TBRmax*SUV bloodpool (1.28)

Study	Patients category	Age (years)	N (% males)	BMI	Method/level of SUV measurement	[¹⁸ F]FDG uptake reported as	[¹⁸ F]FDG uptake VAT	[¹⁸ F]FDG uptake SAT
2015 Tahara et al (7)	CV risk screening male and females	62.6±9.3	251 (69%)	23.7±3.1	ROIs on 11 consecutive slices.	TBR _{max}	0.49±0.10	0.27±0.06
	Male	62.7±9.3	172(100%)	24.2±2.8			0.50±0.09	0.28±0.06
	Female	62.4±9.4	79 (0%)	22.7±3.4			0.49±0.12	0.26±0.07
2015 Oliveira et al (8)	Metabolically healthy/abnormal obese & metabolically healthy lean		141 (49%)		ROIs VAT: largest cross-section of omental SAT: posterolateral	SUV _{mean}		
	Metabolically healthy obese	50.1±14.3	20 (30%)	30.7±5.2			0.46±0.11	0.24±0.06
	Metabolically abnormal obese	57.5±15.5	61 (52%)	32.1±4.5			0.43±0.13	0.24±0.07
	Metabolically healthy lean	49.6±18.9	60 (52%)	23.0±2.6			0.61±0.20	0.26±0.10
2014 Vanfleteren et al (9)	COPD and no COPD subjects	66.6±8.3	42 (71%)	25.1±4.3	ROIs were placed on at least three consecutive slices around the umbilical region.	TBR _{max}		
	No COPD subjects	65.2±8.3	23 (65%)	26.2±4.3			0.28±0.09	0.21±0.09
	COPD subjects	68.4±8.3	19 (79%)	23.7±4.0			0.38±0.18	0.24±0.09
2013 Kodama et al (10)	Impaired glucose tolerance or type 2 diabetes mellitus		53 (75%)		ROIs were placed on the umbilical level and the additional 10 slices.	TBR _{mean}		
	allocated to pioglitazone baseline	68.4±7.3	32 (72%)	25.2±3.5			0.57±0.16	0.30±0.07
	16 weeks of treatment						0.50±0.11	0.29±0.06
	allocated to glimepiride baseline	66.7±9.1	21 (81%)	24.7±3.7			0.54±0.11	0.30±0.06
	16 weeks of treatment				0.58±0.09	0.32±0.06		
2013 Reichkednler et al (11)	Moderate overweight Caucasian males (3 treatment groups)	30±6	61 (100%)	28.1±1.8	Manually predefined cubic and spheric volumes (VOI), placed between Th11-12 and L5/S1.	SUV _{mean}	Only reported in a graph. Between 0.2 and 0.4.	
2013 Vosselman et al(12)	Lean adult man after high calorie meal and after cold exposure	23.6±2.1	11 (100%)	22.4±2.1	Selecting cubes as VOI on the relevant tissue. VAT: behind the xiphoid SAT: L3 - L4	SUV _{mean}		
	After high calorie meal	23.6±2.1	11 (100%)	22.4±2.1			0.49±0.24	0.35±0.15
	After cold exposure		6 (100%)				0.51±0.23	0.18±0.05

Study	Patients category	Age (years)	N (% males)	BMI	Method/level of SUV measurement	[¹⁸ F]FDG uptake reported as	[¹⁸ F]FDG uptake VAT	[¹⁸ F]FDG uptake SAT
2012 Elkhaward et al (13)	Patient with atherosclerosis on stable statin therapy (total)	63.8±6.0	99 (86%)	28.9±3.5	ROI on 5 consecutive slices, close to L2.	SUV _{max}		
	high dose losmapimod baseline	62.3±5.9	34 (85%)	29.8±3.7			0.59±0.11	0.32±0.09
	high dose losmapimod day 84						0.53±0.12	0.30±0.10
	losmapimod lower dose baseline	65.3±5.9	33 (85%)	28.0±3.4			0.58±0.13	0.34±0.09
	losmapimod lower dose day 84						0.56±0.14	0.31±0.08
	placebo baseline	63.7±6.4	32 (88%)	28.9±3.4			0.57±0.13	0.34±0.11
	placebo day 84						0.57±0.08	0.32±0.11
2010 Christen et al (14)	Obese and lean patients staging of primary lung cancer (total)		57 (49%)		ROIs on 25 consecutive slices to create a VOI.	SUV _{mean}		
	Lean patients (BMI < 25 kg/m ²)	66.0±14.8	26 (46%)	21.7±0.6			0.88±0.18	0.30±0.09
	Obese patients (BMI > 30 kg/m ²)	61.4±10.4	31 (52%)	36.4±3.5			0.81±0.22	0.33±0.08

Values are n (%), mean±SD, median and interquartile range.

BMI = Body Mass Index; CT = Computed Tomography; CV = Cardiovascular; COPD = Chronic Obstructive Pulmonary Disease; FDG = ¹⁸F-Fluorodeoxyglucose; HU = Hounsfield Unit;
MGUS = Monoclonal Gammopathy of Undetermined Significance; MM = Multiple Myeloma; MR= Magnetic Resonance Imaging; ROIs = Regions Of Interest; SAT = Subcutaneous Adipose Tissue; SUV =
Standardized Uptake Value; VAT = Visceral Adipose Tissue; VOI = Volume Of Interest

Supplementary Figures

Supplemental Figure 1 : Flowchart study selection

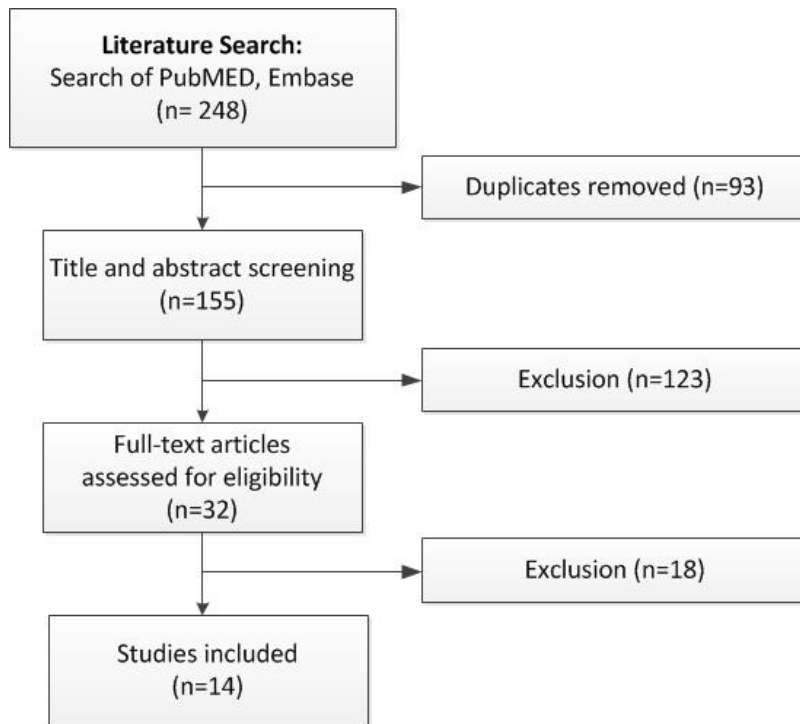


Fig. S1. Flowchart study selection. Reviewing titles and abstract revealed 32 potentially eligible for inclusion. After reviewing the full article, 18 papers were excluded because [^{18}F]FDG uptake was not reported as SUV or only reported of the thoracic visceral adipose tissue or only the visceral fat area or volume was reported and not the [^{18}F]FDG uptake. Eventually, 14 studies met all inclusion.

Supplemental Figure 2: 3D plots of intraclass correlation coefficients for different thresholds and erosions

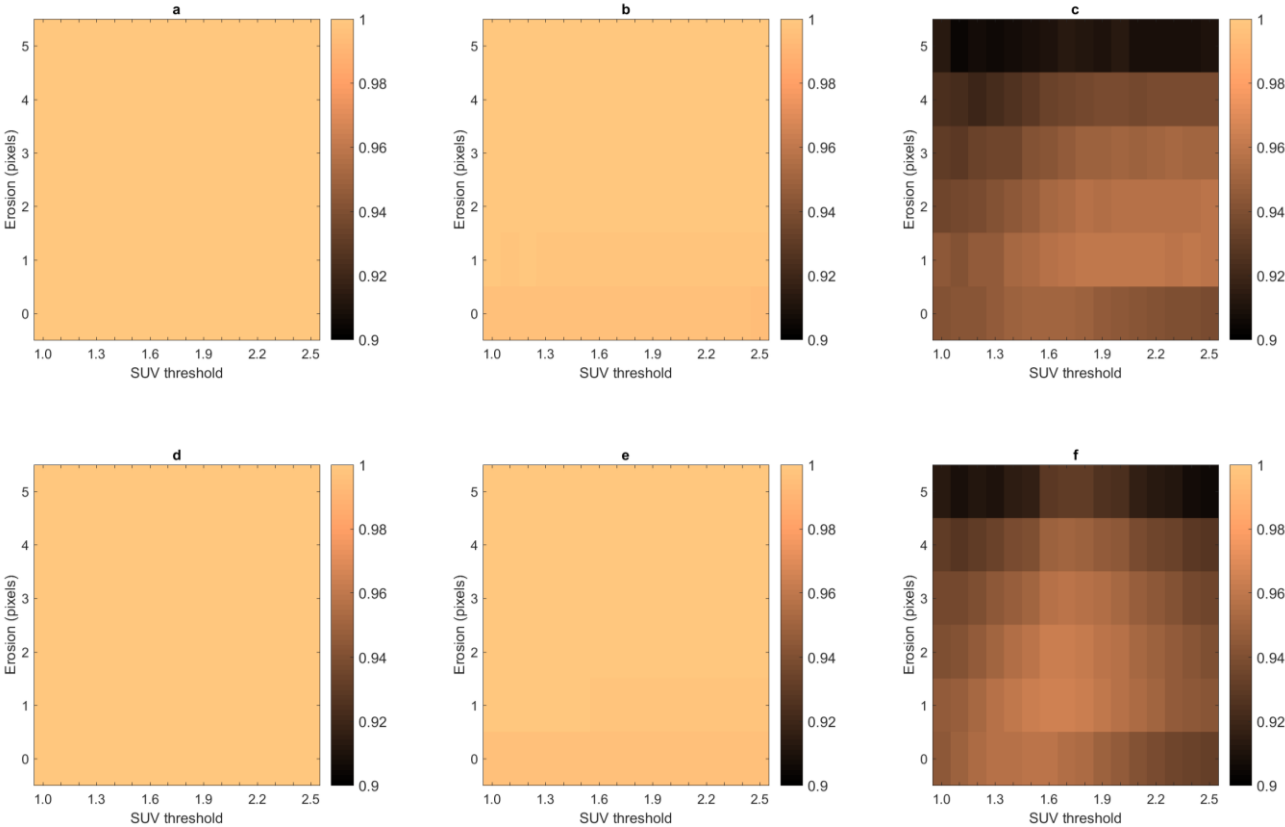


Fig. S2. Each 3D plot represents 96 ICCs calculated for the different SUV thresholds (x-as) and erosions (y-as).
The ICCs for interobserver reproducibility for **a** $^A\text{SUV}_{\text{median}}$ VAT and for **d** $^A\text{SUV}_{\text{mean}}$ VAT. The ICCs for intraobserver reproducibility for **b** $^A\text{SUV}_{\text{median}}$ VAT and for **e** $^A\text{SUV}_{\text{mean}}$ VAT. The repeatability ICCs for **c** $^A\text{SUV}_{\text{median}}$ VAT and for **f** $^A\text{SUV}_{\text{mean}}$ VAT.

Supplemental Figure 3: Distribution of SUV values in VAT and SAT

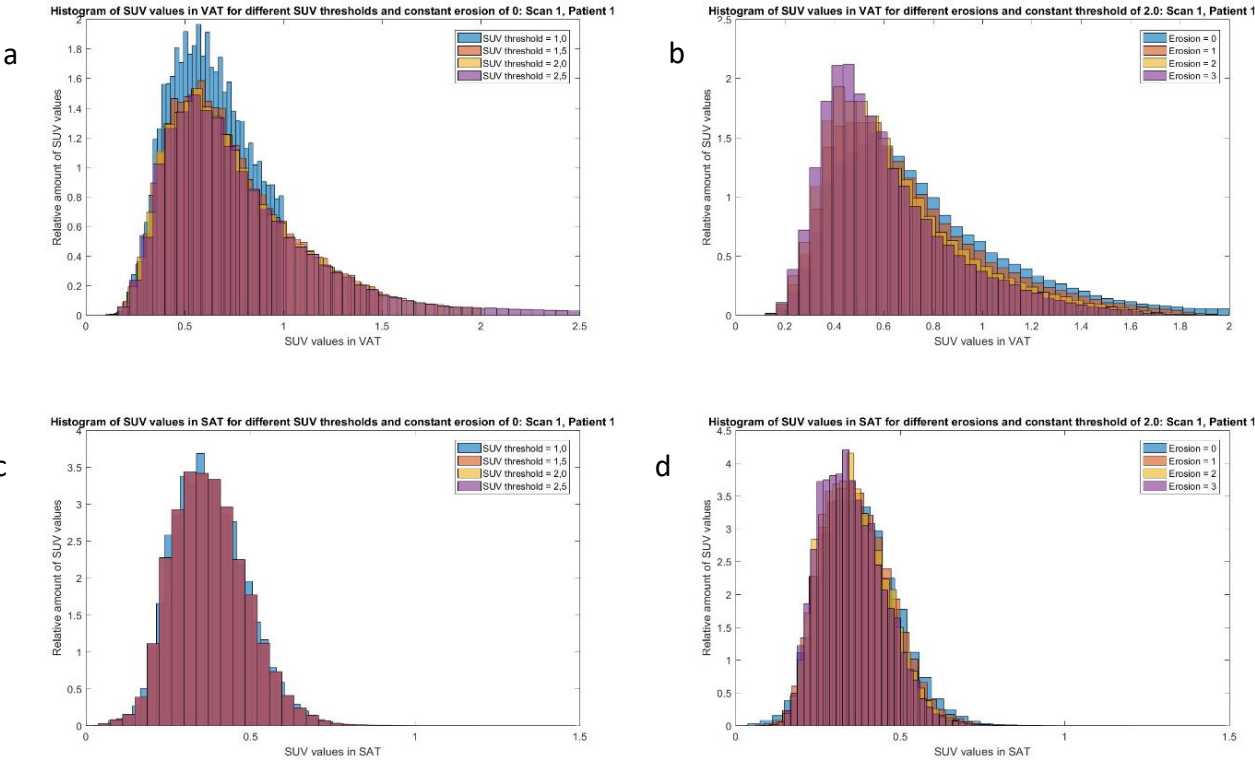


Fig. S3. a Histogram with SUV values in VAT with different SUV thresholds and no erosion and **b** for different erosions and a SUV threshold of 2.0. **c** Histogram with SUV values in SAT with different SUV thresholds and no erosion and **d** for different erosions and a SUV threshold of 2.0.

Supplemental Figure 4: Influence of different SUV threshold on abdominal adipose tissue

Fig. S4. The influence of different SUV threshold on the remaining VAT and SAT (without an erosion).

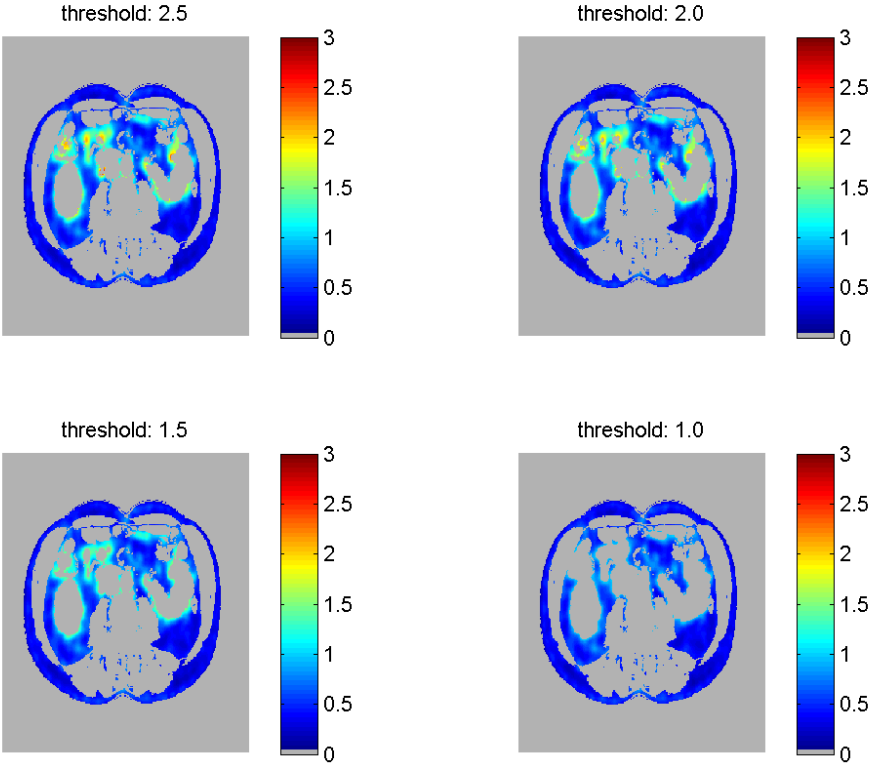


Fig. S4. When the threshold is set at 2.5, there is still some spillover detected in the VAT region. For lower thresholds this spillover, together with SUV values from VAT are removed.

Supplemental Figure 5: Influence of different erosions on abdominal adipose tissue

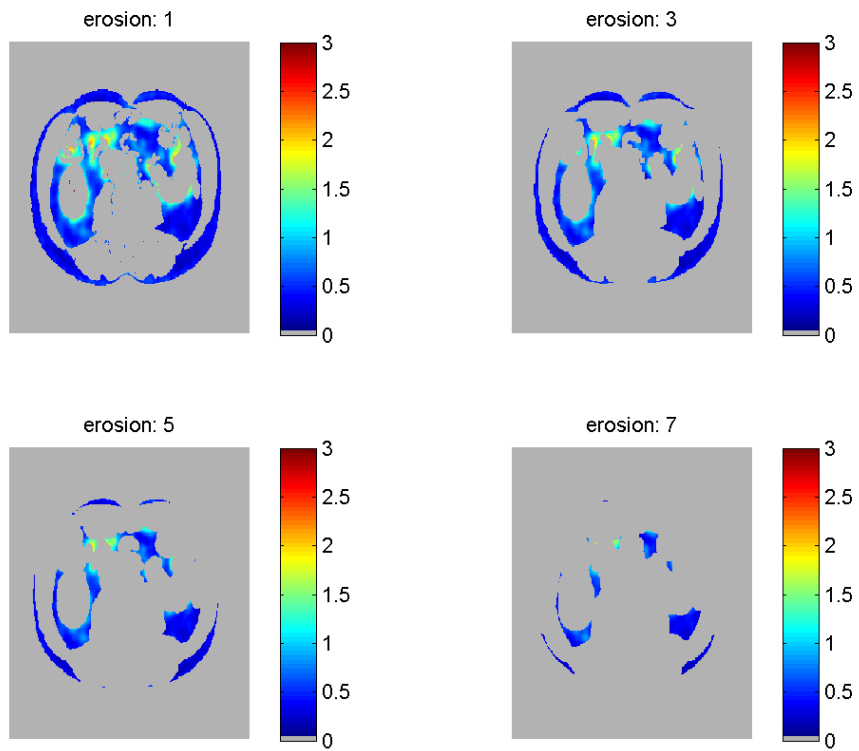


Fig. S5. The influence of different erosions (without a SUV threshold) on the remaining VAT and SAT regions. Most spillover effects are removed for an erosion of 1 pixel. When larger erosions are used also SUV values from VAT and SAT regions are removed.

Supplementary References

1. Torigian DA, Green-McKenzie J, Liu X, Shofer FS, Werner T, Smith CE, Strasser AA, Moghbel MC, Parekh AH, Choi G, Goncalves MD, Spaccarelli N, Gholami S, Kumar PS, Tong Y, Udupa JK, Mesaros C, Alavi A. A Study of the Feasibility of FDG-PET/CT to Systematically Detect and Quantify Differential Metabolic Effects of Chronic Tobacco Use in Organs of the Whole Body-A Prospective Pilot Study. *Acad Radiol* 2016.
2. Van de Wiele C, Van Vlaenderen M, D'Hulst L, Delcourt A, Copin D, De Spiegeleer B, Maes A. Metabolic and morphological measurements of subcutaneous and visceral fat and their relationship with disease stage and overall survival in newly diagnosed pancreatic adenocarcinoma: Metabolic and morphological fat measurements in pancreatic adenocarcinoma. *Eur J Nucl Med Mol Imaging* 2017;44:110-6.
3. Veld J, O'Donnell EK, Reagan MR, Yee AJ, Torriani M, Rosen CJ, Bredella MA. Abdominal adipose tissue in MGUS and multiple myeloma. *Skelet Radiol* 2016;45:1277-83.
4. Pahk K, Rhee S, Kim S, Choe JG. Predictive role of functional visceral fat activity assessed by preoperative F-18 FDG PET/CT for regional lymph node or distant metastasis in patients with colorectal cancer. *PLoS ONE* 2016;11.
5. Im HJ, Paeng JC, Cheon GJ, Kim EE, Lee JS, Goo JM, Kang KW, Chung JK, Lee DS. Feasibility of simultaneous 18F-FDG PET/MRI for the quantitative volumetric and metabolic measurements of abdominal fat tissues using fat segmentation. *Nucl Med Commun* 2016;37:616-22.
6. Bucerius J, Vijgen GHEJ, Brans B, Bouvy ND, Bauwens M, Rudd JHF, Havekes B, Fayad ZA, Van Marken Lichtenbelt WD, Mottaghy FM. Impact of Bariatric Surgery on Carotid Artery Inflammation and the Metabolic Activity in Different Adipose Tissues. *Medicine* 2015;94.
7. Tahara N, Yamagishi S-, Kodama N, Tahara A, Honda A, Nitta Y, Igata S, Matsui T, Takeuchi M, Kaida H, Kurata S, Abe T, Fukumoto Y. Clinical and biochemical factors associated with area and metabolic activity in the visceral and subcutaneous adipose tissues by FDG-PET/CT. *J Clin Endocrinol Metab* 2015;100:E739-47.
8. Oliveira AL, Azevedo DC, Bredella MA, Stanley TL, Torriani M. Visceral and subcutaneous adipose tissue FDG uptake by PET/CT in metabolically healthy obese subjects. *Obesity* 2015;23:286-9.
9. Vanfleteren LEGW, Van Meerendonk AMG, Franssen FM, Wouters EFM, Mottaghy FM, Van Kroonenburgh MJ, Bucerius J. A possible link between increased metabolic activity of fat tissue and aortic wall inflammation in subjects with COPD. A retrospective 18F-FDG-PET/CT pilot study. *Respir Med* 2014;108:883-90.
10. Kodama N, Tahara N, Tahara A, Honda A, Nitta Y, Mizoguchi M, Kaida H, Ishibashi M, Abe T, Ikeda H, Narula J, Fukumoto Y, Yamagishi S-, Imaizumi T. Effects of pioglitazone on visceral fat metabolic activity in impaired glucose tolerance or type 2 diabetes mellitus. *J Clin Endocrinol Metab* 2013;98:4438-45.
11. Reichkender MH, Auerbach P, Rosenkilde M, Christensen AN, Holm S, Petersen MB, Lagerberg A, Larsson HBW, Rostrup E, Mosbeck TH, Sjödin A, Kjaer A, Ploug T, Hoejgaard L, Stallknecht B. Exercise training favors increased insulin-stimulated glucose uptake in skeletal muscle in contrast to adipose tissue: A randomized study using FDG PET imaging. *Am J Physiol Endocrinol Metab* 2013;305:E496; E506.
12. Vosselman MJ, Brans B, Van Der Lans AAJ, Wierts R, Van Baak MA, Mottaghy FM, Schrauwen P, Van Marken Lichtenbelt WD. Brown adipose tissue activity after a high-calorie meal in humans. *Am J Clin Nutr* 2013;98:57-64.
13. Elkhawad M, Rudd JHF, Sarov-Blat L, Cai G, Wells R, Davies LC, Collier DJ, Marber MS, Choudhury RP, Fayad ZA, Tawakol A, Gleeson FV, Lepore JJ, Davis B, Willette RN, Wilkinson IB, Sprecher DL, Cheriyan J. Effects of p38 mitogen-activated protein kinase inhibition on vascular and systemic inflammation in patients with atherosclerosis. *JACC Cardiovasc Imaging* 2012;5:911-22.
14. Christen T, Sheikine Y, Rocha VZ, Hurwitz S, Goldfine AB, Di Carli M, Libby P. Increased glucose uptake in visceral versus subcutaneous adipose tissue revealed by PET imaging. *JACC Cardiovasc Imaging* 2010;3:843-51.